J Biomol NMR (2010) 47:155–162
DOI 10.1007/s10858-010-9417-9

ARTICLE

Comparison of fast backbone dynamics at amide nitrogen and carbonyl sites in dematin headpiece C-terminal domain and its S74E mutant

Liliya Vugmeyster · Dmitry Ostrovsky · Ying Li

Received: 20 January 2010 / Accepted: 29 March 2010 / Published online: 16 April 2010

Abstract We perform a detailed comparison of fast backbone dynamics probed at amide nitrogen versus carbonyl carbon sites for dematin headpiece C-terminal domain (DHP) and its S74E mutant (DHPS74E). Carbonyl dynamics is probed via auto-correlated longitudinal rates and transverse C′/C′-C^{α} CSA/dipolar and C′/C′–N CSA/dipolar cross-correlated rates, while ^{15}N data are taken from a previous study. Resulting values of effective order parameters and internal correlation times support the conclusion that C′ relaxation reports on a different subset of fast motions compared to those probed at N–H bond vectors in the same peptide planes. ^{13}C′ order parameters are on the average 0.08 lower than ^{15}N order parameters with the exception of the flexible loop region in DHP. The reduction of mobility in the loop region upon the S74E mutation can be seen from the ^{15}N order parameters but not from the ^{13}C order parameters. Internal correlation times at ^{13}C′ sites are on the average an order of magnitude longer than those at ^{15}N sites for the well-structured C-terminal subdomains, while the more flexible N-terminal subdomains have more comparable average internal correlation times.

Keywords Dematin headpiece · NMR relaxation · Backbone dynamics · Carbonyl dynamics · Fast motions · Model-free

Introduction

Protein dynamics have been shown to play a role in many biological functions of proteins. (Palmer 2004; Eisenmesser et al. 2005; Mittermaier and Kay 2006; Gardino and Kern 2007). To study the details of the dynamics, many techniques have been developed that probe a variety of time scales and nuclei. (Engelke and Ruterjans 1997; Yang et al. 1998; Brutscher 2000; Palmer 2004; Lundstrom et al. 2005; Mittermaier and Kay 2006; Wang et al. 2006; Yang et al. 2006). The most popular method remains to be the measurements of backbone ^{15}N R_1, R_2, and heteronuclei ^{1}H-^{15}N NOE with the analysis of the data using the model-free approach developed by Lipari and Szabo (1982) and extended by Clore et al. (1990). This approach has yielded many invaluable results and, importantly, has been applied to a large variety of proteins. Thus, it allows for comparison between many different types of proteins and facilitates theoretical/computation studies of general principles governing backbone dynamics. The popularity of this approach is supported by the availability of standard pulse sequences for data collection and computational tools for data analysis (Peng and Wagner 1992; Farrow et al. 1994; Orekhov et al. 1994; Mandel et al. 1995; Cole and Loria 2003).

Electronic supplementary material The online version of this article (doi:10.1007/s10858-010-9417-9) contains supplementary material, which is available to authorized users.

L. Vugmeyster (✉)
Department of Chemistry and Environment and Natural Resources Institute, University of Alaska at Anchorage, 3211 Providence Drive, Anchorage, AK 99508, USA
e-mail: aflv@uaa.alaska.edu

D. Ostrovsky
Department of Mathematical Sciences, University of Alaska at Anchorage, 3211 Providence Drive, Anchorage, AK 99508, USA

Y. Li
Department of Biochemistry & Molecular Biophysics, Columbia University, 630 West 168th Street, New York, NY 10032, USA

^{15}N R_1, R_2, and heteronuclear ^{1}H-^{15}N NOE measurements primarily probe fast ps motions of the N–H bond vector. It has been recognized that the amide N–H bond vector is not sensitive to some modes of motions experienced by the peptide plane, and that additional probes within the peptide plane will provide complimentary information on the dynamics of the plane. In addition, out of the plane motions of amide hydrogen are possible (Mannfors et al. 2003; Ulmer et al. 2003), which have an effect on the ^{15}N relaxation rates. Carbonyl carbon is a good complimentary probe and is not affected by the out of plane motions for the amide hydrogen. However, until recently the variability in its chemical shift anisotropy (CSA) tensor components made it difficult to interpret the variability in the experimental rates measured at carbonyl carbons in terms of the differences in dynamics rather than structural changes. Chang and Tjandra (2005), and Engelke and Ruterjans (1997), have analyzed fast dynamics probed at carbonyl nuclei using a combination of R_1 and R_2 rates at different magnetic fields.

Wang et al. (2006) have undertaken a different approach by looking at a combination of ^{13}C′ R_1, ^{13}C′/^{13}C′-^{13}C$^{\alpha}$ CSA/dipolar and ^{13}C′/^{13}C′–^{15}N CSA/dipolar cross-correlated rates. They have developed a useful computational program, COMFORD, which fits the experimental rates to corresponding spectral densities expressions to obtain effective ^{13}C′ order parameters, local correlation times and directions of ^{13}C′ CSA tensors. The amplitude of local fluctuations for all interactions contributing to the three experimental rates at each site is assumed to be the same, and is thus reflected in a single effective value of the ^{13}C′ order parameter. All three ^{13}C′ relaxation rates are least sensitive to rotational fluctuations about an imaginary C$^{\alpha}$–C$^{\alpha}$ axis, a so-called crank-shaft motions (Bremi and Bruschweiler 1997), and most sensitive to rotational fluctuations about an imaginary axis parallel to the N–H bond direction, a so-called α-axis (Wang et al. 2006). In contrast, the relaxation rates probed on ^{15}N–H bonds are not sensitive to the motions around the α-axis, but rather to the motions around the directions which are perpendicular to this axis. Thus, even if one assumes a perfectly planar peptide plane, different information can be obtained from probing ^{13}C′ nuclei versus N–H bonds motions.

The approach makes use of empirical rules developed by Loth et al. (2005) for the estimation of site-specific variations of ^{13}C′ CSA tensors from isotropic chemical shifts, thus facilitating the separation of structural and dynamic contribution to the experimental rates. These empirical rules, obtained on the basis of fourteen auto and cross-correlated relaxation experiments, confirmed earlier density functional theory calculations (Markwick and Sattler 2004), solid-state NMR data (Gu et al. 1994; Wei et al. 2001), and solution NMR experiments (Cisnetti et al. 2004), which suggested that the σ_{22} components of the ^{13}C′ CSA tensors contain most of the site to site variability in proteins, while the other two components are nearly constant.

By adopting the approach of Wang et al., we perform a comparison of fast backbone dynamics probed at ^{15}N versus ^{13}C′ nuclei for dematin headpiece C-terminal domain and its phosphorylated analog which has the S74E mutation.

Dematin is an actin-binding protein abundant in red blood cells and other tissues (Kim et al. 1998). It contains a villin-type 'headpiece' F-actin-binding domain at its extreme C-terminus. The structure of the C-terminal domain of the dematin headpiece (DHP) was determined by solution NMR (Frank et al. 2004) and is shown in Fig. 1. DHP is composed of a well-folded helical subdomain (residues 41–76), which is very similar to the analogous region in the villin headpiece, and a more mobile N-terminal subdomain (residues 9–40), consisting of mainly loops and turns. The isolated dematin headpiece domain (DHP) undergoes a significant conformational change upon phosphorylation (Frank et al. 2004). The mutation of Ser74 to Glu closely mimics the phosphorylation of DHP (Jiang and McKnight 2006). Previous dynamics studies of these proteins have focused on the analysis of ^{15}N auto-correlated relaxation rates and two cross-correlated rates that yielded information on μs-ms time scales (Jiang and McKnight 2006; Vugmeyster and McKnight 2009). These results indicated a reduction in mobility upon the mutation in several regions of the protein.

In this work we show that fast backbone dynamics of DHP and DHPS74E proteins probed at carbonyl sites are likely to report on different motions compared to those probed at ^{15}N sites, as evidenced by the comparison of the values of the order parameters and local correlation times.

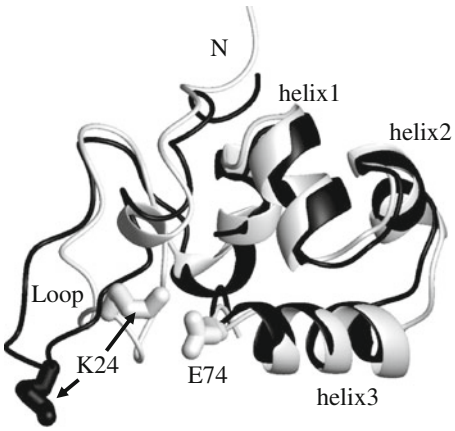

Fig. 1 Structures of DHP (*black*) and DHPS74E (*white*). The side chains of Lys24 and Glu74 that are involved in the salt bridge between the N- and C-terminal subdomains are shown as sticks. This figure was produced with MOLMOL (Koradi et al. 1996)

Materials and methods

Sample preparation

$^{15}N/^{13}C$ labeled DHP and DHPS74E proteins were prepared as described previously (Frank et al. 2004; Jiang and McKnight 2006). NMR samples were prepared in 20 mM sodium phosphate, 0.02% sodium azide, 10% D_2O and adjusted to pH 6.0. Final concentration of the samples were 1.5 mM for DHP and 2.5 mM for DHPS74E.

NMR spectroscopy

All data were collected on a 500 MHz Bruker NMR spectrometer equipped with a triple resonance triple-gradient TXI probe. The temperature was set at 25°C with deuterated methanol sample calibration standard (Findeisen et al. 2007).

$^{13}C'$ R_1 longitudinal relaxation rates were measured by a two-dimensional HN(CO) type pulse sequence (Kay et al. 1990) taking care to suppress cross-correlated mechanisms involving N, H, and C^α nuclei with 180° pulses. Six relaxation delays between 0.01 and 1.4 s were collected. The number of scans used was 32. The relaxation rates were obtained by fitting signal intensities to a mono-exponential decay. The uncertainties in rates were obtained by jack-knife simulations (Mosteller and Tukey 1977).

$^{13}C'/^{13}C'$-$^{13}C^\alpha$ CSA/dipolar ($R_{C'/C'-C\alpha}$) and $^{13}C'/^{13}C'$–^{15}N CSA/dipolar ($R_{C'/C'-N}$) cross-correlated rates were measured using HN(CO) type pulse sequences described in Loth et al. (2005). The experiments are based on the principle of symmetrical reconversions (Pelupessy et al. 2003, 2007). Cross-correlation causes inter-conversions between two operators, in general denoted by P and Q. They are given by C'_y and $2C'_yC^\alpha_z$ operators for the $^{13}C'/^{13}C'$ -$^{13}C^\alpha$ experiment and C'_y and $2C'_yN_z$ operators for the $^{13}C'/^{13}C'$–^{15}N experiment. Four measurements, denoted by I, II, III, and IV, are collected in order to determine each cross-correlated rate. Experiment I measures the decay of P, IV the decay of Q, II the conversion $P \rightarrow Q$, and III the conversion $Q \rightarrow P$. The cross-correlated rate is extracted from the peak volumes of the four interleaved experiments as $|R_{cc}| = \frac{1}{T}\tanh^{-1}\sqrt{\left(\frac{A_{II}A_{III}}{A_IA_{IV}}\right)}$, where T is the relaxation delay time. The sign of the rate is determined by comparing the sign of intensities in the four experiments. The errors in the cross-correlated rates were estimated by assuming that errors in the intensity for each experiment are given by noise level in corresponding spectra. Two data sets were recorded with the relaxation delays of 80 and 60 ms. Data set for 80 ms delay was repeated twice for DHP. Thirty two scans were used for experiments I and IV, and either 64 (C'/C'-C^α) or 128 (C'/C'-N) for experiments II and III.

For all three rates 512 × 40 complex points were collected with the spectral width of 12 and 25 ppm in ^1H and ^{15}N dimensions, respectively. Recycle delay of 1.5 s was used. The data were processed by the NmrPipe/NmrDraw/NlinLS package (Delaglio et al. 1995). Each dimension was apodized by a 90° phase-shifted sine-bell window function and zero-filled once.

Several residues were not included due to either signal overlap or very low initial intensity. Reliable values of at least one of the cross-correlated rates were missing for L19, D34, R37, and D46 in DHP and R37, D46, and A62 in DHPS74E.

Determination of $^{13}C'$ order parameters

COMFORD program (Wang et al. 2006) was used to obtain the values of $^{13}C'$ order parameters, effective local correlation times and the orientation of the $^{13}C'$ CSA tensors. In addition to the R_1, $R_{C'/C'-C\alpha}$, and $R_{C'/C'-N}$ relaxation rates, the program requires isotropic $^{13}C'$ chemical shifts as an input and uses the rules developed by Loth et al. (2005) for the calculations of the components of the $^{13}C'$ CSA tensors. $^{13}C'$ assignments were taken from Frank et al. (2004) and Jiang et al. (2006). COMFROD gives most accurate fits when the molecular tumbling times are taken from ^{15}N relaxation measurements. Our previous analysis of ^{15}N relaxation data has shown that the assumption of isotropic tumbling is a reasonable approximation as the diffusion tensor anisotropy was shown to be small in both proteins. The values of molecular tumbling times τ_c are 5.2 ns for DHP and 5.7 ns for DHPS74E (Vugmeyster and McKnight 2009).

To parameterize the experimental rates COMFORD uses the following spectral density expression which assumes identical order parameters S^2 for any two interactions a and b:

$$J^{ab} = \frac{2}{5}\left(\frac{S^2\tau_c}{1+(\omega\tau_c)^2} + \frac{(1-S^2)\tau}{1+(\omega\tau)^2}\right)P_2(\cos\theta^{ab}) \quad (1)$$

For auto-correlated terms $a = b$. P_2 is the second order Legendre polynomial and θ^{ab} is the angle between chosen components of the two interactions. $\tau = \frac{\tau_c\tau_e}{\tau_c+\tau_e}$, where τ_e reflects an average of local motions affecting a and b simultaneously. The interaction angles relevant to $R_{C'/C'-C\alpha}$ differ from angles relevant to the $R_{C'/C'-N}$ by the C^α–C'–N bond angle of 117°. We discuss the limits of the validity of (1), as well as the dependence of the order parameters on the choice of the CSA tensor components in Supporting Information S1 and S2.

The expression for the rates in terms of the spectral densities are given in references (Goldman 1984; Boyd et al. 1991; Brutscher et al. 1998; Fischer et al. 1998; Wang et al. 2006). COMFORD uses a convention with an inverted sign for the cross-correlated rates and, therefore, for the fitting purpose we switched the sign in the experimental cross-correlated rates.

If several reasonable fits are possible, COMFORD selects the most robust one, where a variation in experimental data within the limits of error would not eliminate the fit. COMFORD algorithm did not converge for carbonyls of residues M36 in both proteins.

Results and discussion

Experimental rates for DHP and DHPS74E are shown in Fig. 2. The values of $R_{C'/C'-C\alpha}$ and $R_{C'/C'-N}$ cross-correlated rates obtained using 60 and 80 ms relaxation delays showed a good agreement between each other. Larger errors for the loop region are due to smaller peak volumes.

As elaborated in the Materials and Methods section, COMFORD fits the three experimental rates against corresponding theoretical expressions for the rates with the use of the spectral density function defined by (1), parameterized by the effective motional order parameter S^2, effective internal correlation time τ_e and the angle θ representing the orientation of σ_{11} axis (least shielded component) of $^{13}C'$ CSA tensor with respect to the C′-C$^{\alpha}$ bond vector.

Since our main goal is to compare ^{15}N and $^{13}C'$ dynamics of the same peptide plane, we will adopt residue numbering corresponding to ^{15}N sites.

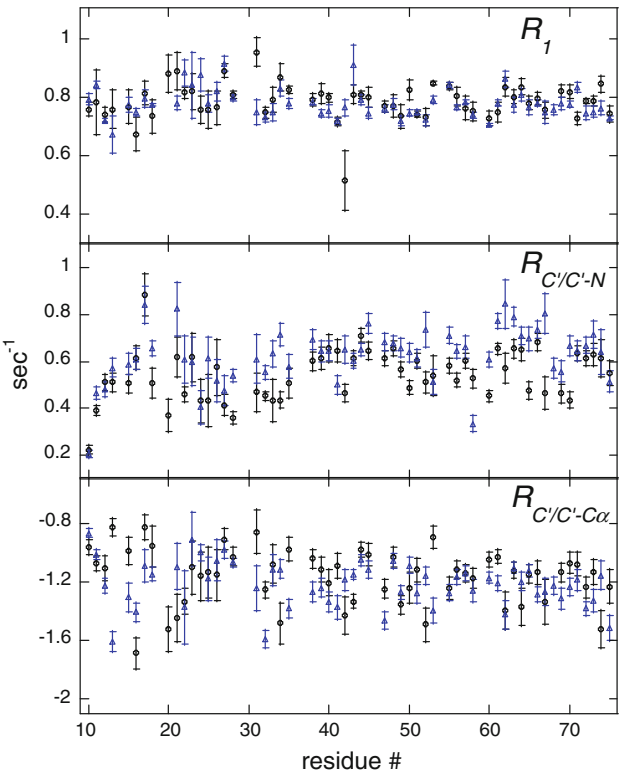

Fig. 2 $^{13}C'$ R_1, $R_{C'/C'-C\alpha}$ and $R_{C'/C'-N}$ rates for DHP (*black circles*) and DHPS74E (*blue triangles*) for 80 ms relaxation delay. Residue numbering is by the carbonyls

Analysis of the order parameters

Figure 3 shows the order parameters at ^{15}N and $^{13}C'$ sites obtained from COMFORD output for the two proteins. The most apparent feature of the comparison in the order parameters is that their values for the $^{13}C'$ sites are in general lower and display a larger variability than those for the ^{15}N sites in the same peptide plane. The exception is the flexible loop region, residues 20-30, which was shown

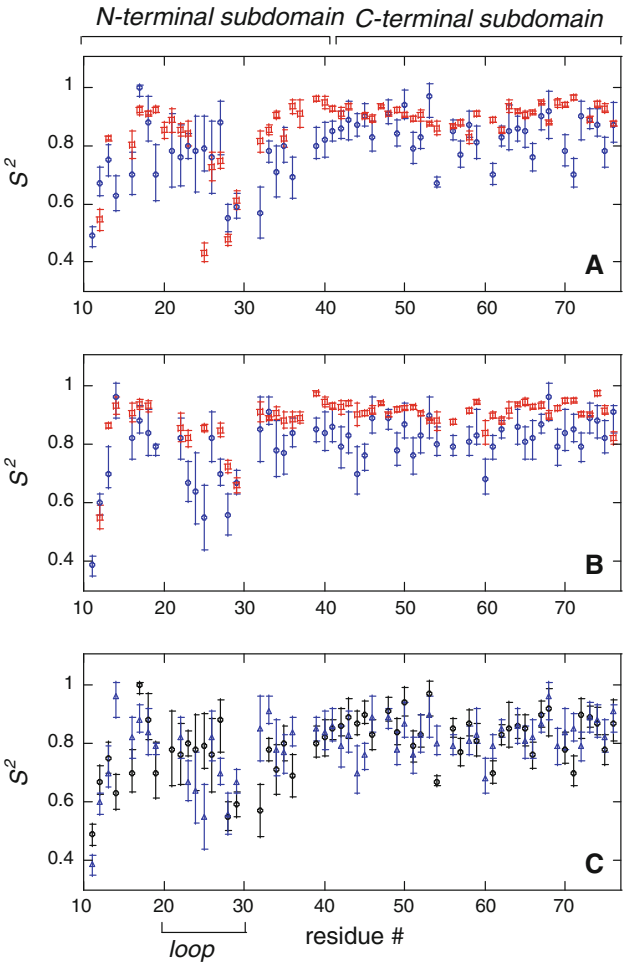

Fig. 3 Order parameters at **a** ^{15}N (*red squares*) and $^{13}C'$ (*blue circles*) sites for DHP; **b** ^{15}N (*red squares*) and $^{13}C'$ (*blue circles*) sites for DHPS74E; **c** $^{13}C'$ for DHP (*black circles*) and DHPS74E (*blue triangles*). Residue numbering is by ^{15}N. Amide nitrogen order parameters were taken from an earlier study. (Vugmeyster and McKnight 2009)

to be very flexible in the DHP by ^{15}N studies. While in this region the values of the carbonyl order parameters tend to be lower than in the structured part of the protein, they are on the average not lower than those probed by ^{15}N relaxation (Fig. 3a). Excluding the loop region, the average difference $S^2(^{15}\mathrm{N})$-$S^2(^{13}\mathrm{C}')$ is 0.076.

In DHPS74E the mobility of N–H bond vectors for the flexible loop was shown to be reduced in comparison to DHP. This trend can not be seen by looking at the carbonyl order parameters only (Fig. 3c), which suggests that the motions in the loop region of DHP are highly anisotropic. ^{15}N versus $^{13}\mathrm{C}'$ comparison (Fig. 3b) shows that most of the detected residues in the loop region have lower order parameters at carbonyl sites. The average difference $S^2(^{15}\mathrm{N})$-$S^2(^{13}\mathrm{C}')$ is 0.079 excluding the loop region and 0.081 including the loop region.

One of the possible explanations for the observed difference between carbonyl and nitrogen order parameters could stem from the fact that a more rigorous equation for the cross-correlated rates should contain a distribution of angles θ in the spectral density given by (1). This distribution stems from the presence of distribution of conformations, each of which has a slightly different tensor orientation. These conformations can interconvert on a slow μs-ms time scale and their only effect on the spectral density is through the replacement of P_2 $(\cos\theta^{ab})$ in (1) by $<P_2$ $(\cos\theta^{ab})>$, where angular brackets represent conformational average. If this distribution is not included, we expect the effective order parameter to be somewhat smaller (Pelupessy et al. 2003; Vugmeyster et al. 2004; Vugmeyster and McKnight 2008). To estimate the magnitude of this effect we modified the fitting procedure to allow for a Gaussian distribution of angles θ with the width of 10°, which, as we show in the *$^{13}C'$ tensors orientations* section, is a typical variation of the angle throughout the sequence. The correction to the effective order parameters is 1% on the average and less than 3% for all residues. Therefore, this effect can not account for the observed difference in the order parameters.

Thus it appears that carbonyl order parameters report on a different subset of fast motions compared to those probed at ^{15}N sites. These results are consistent with the ones observed for ubiquitin, ribonuclease binase, and calmodulin proteins (Pang et al. 2002; Wang et al. 2003, 2005, 2006), as well as for ribonuclease T1 (Engelke and Ruterjans 1997). Higher correlation between $^{13}\mathrm{C}'$ and ^{15}N order parameters was seen by Chang and Tjandra (2005) for ubiquitin. Interestingly, in ribonuclease T1, binase, and calmodulin $^{13}\mathrm{C}'$ order parameters have been also reported to be lower on the average compared to the ^{15}N order parameters, while ubiquitin $^{13}\mathrm{C}'$ order parameters obtained by the means of COMFORD routine have been shown to be larger than the corresponding ^{15}N order parameters. In addition, $^{13}\mathrm{C}'$ order parameters have displayed a remarkably strong temperature dependence in ubiquitin (Wang et al. 2003), unlike ^{15}N order parameters.

Molecular dynamics simulation conducted for ribonuclease binase (Pang et al. 2002) highlighted interesting features in the comparison of various approaches for dynamics studies: fast motions in two loops predicted by molecular dynamics and reflected in X-ray B-factors were not visible via ^{15}N dynamics, but one of the mobile loops also appeared flexible via $^{13}\mathrm{C}'$ studies. The authors suggest that some of the differences could be attributed to the fact that while NMR relaxation samples exclusively rotations, molecular dynamics is sensitive to translational displacements.

Collectively, these results imply different local potential governing fast fluctuations of N–H bond vectors versus the fluctuations of other atoms in peptide plane. Additional studies of comparative temperature dependence of the order parameters would be helpful to characterize in more details the differences in these potentials.

Analysis of internal correlation times

While comparing local correlation times at ^{15}N and $^{13}\mathrm{C}'$ sites, we have to keep in mind that the model-free procedure for the fits of ^{15}N relaxation data allows for models in which local correlation times τ_e are fixed at zero values (Mandel et al. 1995). Models with non-zero τ_e values are used only for those residues for which there is a statistically significant improvement in the fits due to inclusion of the τ_e fitting parameter. Thus, as can be seen from Fig. 4, there are quite a number of residues for which τ_e at ^{15}N sites are reported as zeros. The majority of these residues are in the C-terminal subdomain. Almost none of the residues have $^{13}\mathrm{C}'$ τ_e values sufficiently close to zero (Fig. 4), therefore for $^{13}\mathrm{C}'$ data fitting we have not explored the model for which the correlation times are fixed at zero.

For a number of residues the COMFORD algorithm yields the values of τ_e exactly at the upper boundary set by $\tau_e = \tau_c/2$ and the uncertainty is very large (Fig. 4). Clearly these values are unreliable as estimates of τ_e. In order to check the sensitivity of the order parameters to the upper boundary of τ_e, we have modified the fitting procedure to change the boundary condition to $\tau_e = \tau_c/5$ and analyzed the values of the resulting order parameters. The order parameters appear to be very robust to such variations in τ_e: the change in S^2 is smaller than 1% on the average and is never larger than 2.5% for all residues in both proteins with the limiting values of τ_e. We thus conclude that even though these residues have to be excluded from a quantitative analysis of internal correlation times, the order parameters reported in Fig. 3 are reliable.

It is interesting that the variability in the ^{15}N internal correlation times between the flexible N-terminal

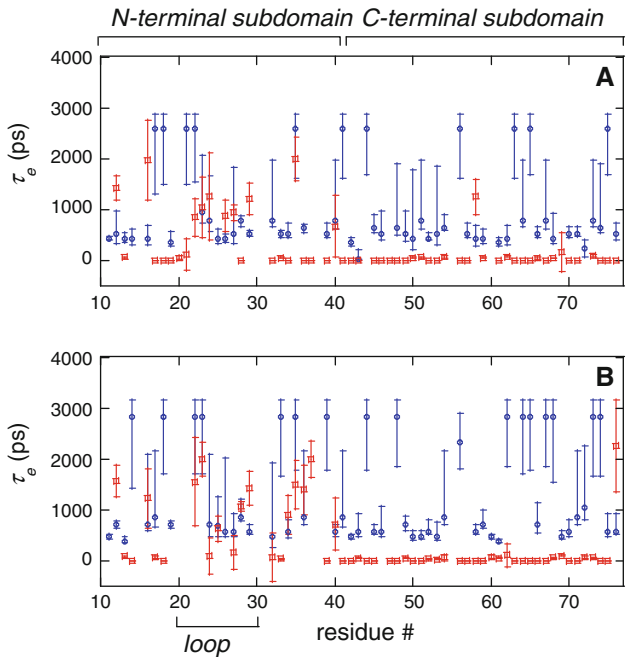

Fig. 4 Internal correlation times at ^{15}N (*red squares*) and ^{13}C′ (*blue circles*) sites for **a** DHP and **b** DHPS74E. Residue numbering is by ^{15}N

subdomain and the more rigid C-terminal subdomain is much larger than the variability for ^{13}C′ correlation times. This already implies a different subset of motions for N–H bond vectors compared to the carbonyl sites. The average values of internal correlation times for the two subdomains are given in Table 1. Average values in the N-terminal subdomains are comparable in ^{15}N versus ^{13}C′ sites, while those for the C-terminal subdomains are almost an order of magnitude larger for the ^{13}C sites.

Surprisingly, for a number of adjacent residues there appears to be a jump in the time scale of dynamics from about 400–700 ps range to over 1 ns range. To check whether this is an artifact of the fitting procedure, specifically whether a false minimum is selected, we have attempted to fit all residues with the upper boundary of $\tau_e = 600$ ps. For those residues in Fig. 4 which show high internal correlation times, the quality of the fits drastically deteriorates, as indicated by χ^2 values (S3). In addition, statistical information provided by COMFORD output did not show any evidence of the presence of multiple minima for any residue. Thus, the jumps of the time scale appear to be real.

Table 1 Average internal correlation times (ps) for the N and C-terminal subdomains at carbonyl and amide nitrogen sites

	N-terminal	C-terminal
^{15}N DHP	520	59
^{13}C′ DHP	570	520
^{15}N DHPS74E	840	89
^{13}C′ DHPS74E	640	690

The residues with limiting values of $\tau_e = \tau_c/2$ are excluded from the analysis

The works by Wang et al. (2006) and Engelke et al. (1997) on ubiquitin, Ca^{2+} saturated calmodulin, and ribonuclease T1 support the conclusion that for well-structured regions ^{13}C′ internal correlation times appear to be much higher on the average compared to those obtained from ^{15}N relaxation. Flexible loop regions have comparable internal correlation times at both sites in calmodulin. The correlation times reported by Chang and Tjandra (2005) for ubiquitin ^{13}C′ sites are slightly larger than those for ^{15}N, but these values are not as large as those reported by Engelke et al. Average values of internal correlation times in DHP and DHPS74E are 540 and 630 ps, respectively. These are in good agreement with the average values for ubiquitin, calmodulin, and ribonuclease T1 of 550, 500, and 350 ps.

Estimation of corrections to the Lipari-Szabo decoupling approximation

The model-free formalism of Lipari and Szabo (1982) assumes that the internal motions are completely independent from the overall molecular tumbling, meaning that in the molecular frame internal motions are completely insensitive to the molecular tumbling. While this model has been proven to be very useful in the analysis of the ^{15}N relaxation, more rigorous analysis has shown that this assumption leads to an overestimation in the values of the order parameters (Tugarinov et al. 2001; Vugmeyster et al. 2003). In the later paper it has been shown that the effect of correlations between internal and overall motions leads to the upper limit of the error in the estimation of the order parameter as $\tau_c/(\tau_c - \tau_e)$. The larger is the ratio τ_e/τ_c the larger is the error. Thus, if ^{13}C internal correlation times for the majority of residues in well-structured regions are larger than those of ^{15}N, the errors are expected to be larger for the ^{13}C order parameters. Average τ_e/τ_c ratios in ubiquitin, DHP, and DHPS74E are 0.12, 0.10, and 0.11, respectively. This yields the maximum corrections of 14, 11 and 12% for ubiquitin, DHP, and DHPS74E. Although real corrections are likely to be somewhat smaller due to a combination of processes involving both correlated and fully decoupled overall tumbling and internal fluctuations, it is clear that the time scales of motions at carbonyl sites are large enough to suspect the necessity of the corrections to the order parameters obtained via the Lipari and Szabo approach. Note, that these corrections would strengthen the conclusions reached in the previous section that ^{13}C′ order

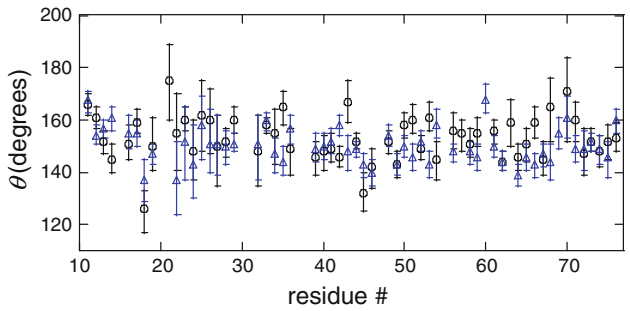

Fig. 5 Angles θ between the least shielded (σ_{11}) components of $^{13}C'$ CSA tensors and C^{α}–C′ bond for DHP (*black circles*) and DHPS74E (*blue triangles*). Residue numbering is by ^{15}N

parameters are lower than ^{15}N order parameters for the well-structured regions.

$^{13}C'$ tensors orientations

The output of the COMFORD for the angle θ is given in Fig. 5. The values are comparable between the two proteins and the averages (standard deviations) are 153(9) for DHP and 150(7) for DHPS74E. These values are in good agreement with those obtained for ubiquitin 154.4 (3.3) by Loth et al. (2005) and 154.6(4.8) by Wang et al. (2006), as well as with 153.8(8.8) for calmodulin.

Conclusion

We have compared fast backbone dynamics at ^{15}N and $^{13}C'$ sites in DHP and DHPS74E proteins based on Lipari-Szabo model-free analysis of ^{15}N R_1, R_2, NOE relaxation rates obtained previously and $^{13}C'$ R_1, $R_{C'/C'-C\alpha}$, and $R_{C'/C'-N}$ relaxation rates obtained in this study. COMFORD fitting routine developed by Zuiderweg and coworkers has been used to analyze the $^{13}C'$ data. Resulting effective $^{13}C'$ order parameters are on the average about 0.08 lower than ^{15}N order parameters with the exception of the flexible loop region in DHP. The reduction of mobility in the loop region (residues 20-30) upon the S74E mutation is obvious from the ^{15}N data but can not be discerned from $^{13}C'$ order parameters, which suggests highly anisotropic fast backbone motions in this region of the protein. Specifically, while the motions around the α-axis are similar in the loop region of both proteins, the motions perpendicular to this direction are more pronounced in the wild-type protein. Internal correlation times at ^{13}C sites are an order of magnitude longer than those at ^{15}N sites for residues in the well-structured C-terminal subdomains, while the more flexible N-terminal subdomains have comparable average internal correlation times at nitrogen and carbonyl sites. The variability in the internal correlation times for the N-terminal subdomains residues appears to be much larger at the N–H vectors compared to those at $^{13}C'$ nuclei.

Our results indicate that $^{13}C'$ relaxation reports on a different subset of fast motions compared to those probed by N–H bond vectors in the same peptide planes. This conclusion is in agreement with most studies of ubiquitin, ribonuclease T1, ribonuclease binase, and Ca^{2+} saturated calmodulin and is consistent with the view that carbonyl carbons and N–H bond vectors are sensitive to motions around different axes. The fact that the internal correlation times for well-structured regions at $^{13}C'$ sites can be an order of magnitude larger than those at ^{15}N sites suggests that the Lipari-Szabo decoupling approximation for the independence of the overall and internal dynamics may be less applicable to $^{13}C'$ dynamics. As a result, the order parameters obtained for $^{13}C'$ sites using the decoupling approximation can be overestimated.

Acknowledgments We are indebted to Prof. C. James McKnight for providing the protein samples and to Prof. Arthur G. Palmer for providing spectrometer time. We are grateful to Prof. Erik Zuiderweg for an access to the COMFORD program and to Dr. Philippe Pelupessy for the guidance on the cross-correlated relaxation pulse sequences. LV acknowledges University of Alaska funds 104110-11970&11470.

References

Boyd J, Hommel U, Krishnan VV (1991) Influence of cross-correlation between dipolar and chemical-shift anisotropy relaxation mechanisms upon the transverse relaxation rates of N-15 in macromolecules. Chem Phys Lett 187:317–324

Bremi T, Bruschweiler R (1997) Locally anisotropic internal polypeptide backbone dynamics by NMR relaxation. J Am Chem Soc 119:6672–6673

Brutscher B (2000) Principles and applications of cross-correlated relaxation in biomolecules. Concepts Magn Reson 12:207–229

Brutscher B, Skrynnikov NR, Bremi T, Bruschweiler R, Ernst RR (1998) Quantitative investigation of dipole-CSA cross-correlated relaxation by ZQ/DQ spectroscopy. J Magn Reson 130:346–351

Chang SL, Tjandra N (2005) Temperature dependence of protein backbone motion from carbonyl C-13 and amide N-15 NMR relaxation. J Magn Reson 174:43–53

Cisnetti F, Loth K, Pelupessy P, Bodenhausen G (2004) Determination of chemical shift anisotropy tensors of carbonyl nuclei in proteins through cross-correlated relaxation in NMR. Chemphyschem 5:807–814

Clore GM, Szabo A, Bax A, Kay LE, Driscoll PC, Gronenborn AM (1990) Deviations from the simple 2-parameter model-free approach to the interpretation of N-15 nuclear magnetic-relaxation of proteins. J Am Chem Soc 112:4989–4991

Cole R, Loria JP (2003) FAST-Modelfree: a program for rapid automated analysis of solution NMR spin-relaxation data. J Biomol NMR 26:203–213

Delaglio F, Grzesiek S, Vuister GW, Zhu G, Pfeifer J, Bax A (1995) NMRPipe: a multidimensional spectral processing system based on UNIX pipes. J Biomol NMR 6:277–293

Eisenmesser EZ, Millet O, Labeikovsky W, Korzhnev DM, Wolf-Watz M, Bosco DA, Skalicky JJ, Kay LE, Kern D (2005) Intrinsic dynamics of an enzyme underlies catalysis. Nature 438:117–121

Engelke J, Ruterjans H (1997) Backbone dynamics of proteins derived from carbonyl carbon relaxation times at 500, 600 and 800 MHz: application to ribonuclease T1. J Biomol NMR 9:63–78

Farrow NA, Muhandiram R, Singer AU, Pascal SM, Kay CM, Gish G, Shoelson SE, Pawson T, Forman-Kay JD, Kay LE (1994) Backbone dynamics of a free and phosphopeptide-complexed Src homology 2 domain studied by 15 N NMR relaxation. Biochemistry 33:5984–6003

Findeisen M, Brand T, Berger S (2007) A H-1-NMR thermometer suitable for cryoprobes. Magn Reson Chem 45:175–178

Fischer MWF, Majumdar A, Zuiderweg ERP (1998) Protein NMR relaxation: theory, applications and outlook. Prog Nucl Magn Reson Spectrosc 33:207–272

Frank BS, Vardar D, Chishti AH, McKnight CJ (2004) The NMR structure of dematin headpiece reveals a dynamic loop that is conformationally altered upon phosphorylation at a distal site. J Biol Chem 279:7909–7916

Gardino AK, Kern D (2007) Functional dynamics of response regulators using NMR relaxation techniques. Methods Enzymol 423:149–156

Goldman M (1984) Interference effects in the relaxation of a pair of unlike spin-1/2 nuclei. J Magn Reson 60:437–452

Gu ZT, Zambrano R, McDermott A (1994) Hydrogen-bonding of carboxyl groups in solid-state amino-acids and peptides—comparison of carbon chemical shielding, infrared frequencies, and structures. J Am Chem Soc 116:6368–6372

Jiang ZG, McKnight CJ (2006) A phosphorylation-induced conformation change in dematin headpiece. Structure 14:379–387

Kay LE, Ikura M, Tschudin R, Bax A (1990) 3-dimensional triple-resonance NMR-spectroscopy of isotopically enriched proteins. J Magn Reson 89:496–514

Kim AC, Azim AC, Chishti AH (1998) Alternative splicing and structure of the human erythroid dematin gene. Biochim Biophys Acta 1398:382–386

Koradi R, Billeter M, Wuthrich K (1996) MOLMOL: a program for display and analysis of macromolecular structures. J Mol Graphics 14:51–55

Lipari G, Szabo A (1982) Model-free approach to the interpretation of nuclear magnetic-resonance relaxation in macromolecules. 1. Theory and range of validity. J Am Chem Soc 104:4546–4559

Loth K, Pelupessy P, Bodenhausen G (2005) Chemical shift anisotropy tensors of carbonyl, nitrogen, and amide proton nuclei in proteins through cross-correlated relaxation in NMR spectroscopy. J Am Chem Soc 127:6062–6068

Lundstrom P, Mulder FAA, Akke M (2005) Correlated dynamics of consecutive residues reveal transient and cooperative unfolding of secondary structure in proteins. Proc Natl Acad Sci USA 102:16984–16989

Mandel AM, Akke M, Palmer AG (1995) Backbone dynamics of escherichia-coli ribonuclease Hi—Correlations with Structure and Function in an Active Enzyme. J Mol Biol 246:144–163

Mannfors BE, Mirkin NG, Palmo K, Krimm S (2003) Analysis of the pyramidalization of the peptide group nitrogen: implications for molecular mechanics energy functions. J Phys Chem A 107:1825–1832

Markwick PRL, Sattler M (2004) Site-specific variations of carbonyl chemical shift anisotropies in proteins. J Am Chem Soc 126: 11424–11425

Mittermaier A, Kay LE (2006) Review—New tools provide new insights in NMR studies of protein dynamics. Science 312:224–228

Mosteller F, Tukey JW (1977) Data analysis and regression: a second course in statistics. Addison-Wesley, Reading

Orekhov VY, Pervushin KV, Arseniev AS (1994) Backbone dynamics of (1–71) bacterioopsin studied by 2-dimensional H-1-N-15 NMR-spectroscopy. Eur J Biochem 219:887–896

Palmer AG (2004) NMR characterization of the dynamics of biomacromolecules. Chem Rev 104:3623–3640

Pang Y, Buck M, Zuiderweg ERP (2002) Backbone dynamics of the ribonuclease binase active site area using multinuclear (N-15 and (CO)-C-13) NMR relaxation and computational molecular dynamics. Biochemistry 41:2655–2666

Pelupessy P, Ravindranathan S, Bodenhausen G (2003) Correlated motions of successive amide N-H bonds in proteins. J Biomol NMR 25:265–280

Pelupessy P, Ferrage F, Bodenhausen G (2007) Accurate measurement of longitudinal cross-relaxation rates in nuclear magnetic resonance. J Chem Phys 126:134508

Peng JW, Wagner G (1992) Mapping of spectral density-functions using heteronuclear NMR relaxation measurements. J Magn Reson 98:308–332

Tugarinov V, Liang ZC, Shapiro YE, Freed JH, Meirovitch E (2001) A structural mode-coupling approach to N-15 NMR relaxation in proteins. J Am Chem Soc 123:3055–3063

Ulmer TS, Ramirez BE, Delaglio F, Bax A (2003) Evaluation of backbone proton positions and dynamics in a small protein by liquid crystal NMR spectroscopy. J Am Chem Soc 125:9179–9191

Vugmeyster L, McKnight CJ (2008) Slow motions in chicken villin headpiece subdomain probed by cross-correlated NMR relaxation of amide NH bonds in successive residues. Biophys J 95:5941–5950

Vugmeyster L, McKnight CJ (2009) Phosphorylation-induced changes in backbone dynamics of the dematin headpiece C-terminal domain. J Biomol NMR 43:39–50

Vugmeyster L, Raleigh DP, Palmer AG, Vugmeister BE (2003) Beyond the decoupling approximation in the model free approach for the interpretation of NMR relaxation of macromolecules in solution. J Am Chem Soc 125:8400–8404

Vugmeyster L, Pelupessy P, Vugmeister BE, Abergel D, Bodenhausen G (2004) Cross-correlated relaxation in NMR of macromolecules in the presence of fast and slow internal dynamics. C R Phys 5:377–386

Wang TZ, Cai S, Zuiderweg ERP (2003) Temperature dependence of anisotropic protein backbone dynamics. J Am Chem Soc 125: 8639–8643

Wang TZ, Frederick KK, Igumenova TI, Wand AJ, Zuiderweg ERP (2005) Changes in calmodulin main-chain dynamics upon ligand binding revealed by cross-correlated NMR relaxation measurements. J Am Chem Soc 127:828–829

Wang T, Weaver DS, Cai S, Zuiderweg ERP (2006) Quantifying Lipari–Szabo modelfree parameters from 13CO NMR relaxation experiments. J Biomol NMR 36:79–102

Wei YF, Lee DK, Ramamoorthy A (2001) Solid-state C-13 NMR chemical shift anisotropy tensors of polypeptides. J Am Chem Soc 123:6118–6126

Yang DW, Mittermaier A, Mok YK, Kay LE (1998) A study of protein side-chain dynamics from new H-2 auto-correlation and C-13 cross-correlation NMR experiments: application to the N-terminal SH3 domain from drk. J Mol Biol 276:939–954

Yang A, Miron S, Mouawad L, Duchambon P, Bloquit Y, Craescu CT (2006) Flexibility and plasticity of human centrin 2 binding to the xeroderma pigmentosum group c protein (XPC) from nuclear excision repair. Biochemistry 45:3653–3663